Inhibition of the Mitogen-Activated Protein Kinase Kinase Superfamily by a *Yersinia* Effector

Kim Orth,[1] Lance E. Palmer,[2]* Zhao Qin Bao,[1] Scott Stewart,[1] Amy E. Rudolph,[1]† James B. Bliska,[2,3] Jack E. Dixon[1]‡

The bacterial pathogen *Yersinia* uses a type III secretion system to inject several virulence factors into target cells. One of the *Yersinia* virulence factors, YopJ, was shown to bind directly to the superfamily of MAPK (mitogen-activated protein kinase) kinases (MKKs) blocking both phosphorylation and subsequent activation of the MKKs. These results explain the diverse activities of YopJ in inhibiting the extracellular signal–regulated kinase, c-Jun amino-terminal kinase, p38, and nuclear factor kappa B signaling pathways, preventing cytokine synthesis and promoting apoptosis. YopJ-related proteins that are found in a number of bacterial pathogens of animals and plants may function to block MKKs so that host signaling responses can be modulated upon infection.

The bacterial pathogen *Yersinia pestis* is the agent of the bubonic plague (*1*). In addition to *Y. pestis*, two closely related species, *Y. enterocolitica* and *Y. pseudotuberculosis*, harbor a plasmid of ~70 kb that encodes a contact-dependent type III secretion system. Upon infection, this system delivers virulence factors (referred to as *Yersinia* outer proteins, or "Yops") into host cells. The Yops disrupt host signaling functions to thwart the development of a cell-mediated immune response (*1*). A virulence factor from *Y. pseudotuberculosis*, YopJ (*2–4*) [YopP in *Y. enterocolitica* (*5*)], is a 33-kD protein that perturbs a multiplicity of signaling pathways. These include inhibition of the extracellular signal–regulated kinase (ERK), c-Jun NH_2-terminal kinase (JNK), and p38 mitogen-activated protein kinase (MAPK) pathways and inhibition of the nuclear factor kappa B (NF-κB) pathway (*2, 6–10*). The interruption of these signaling pathways results in the disruption of tumor necrosis factor α and interleukin-8 production by the infected target cell (*2, 7, 8*). Furthermore, the expression of YopJ has been correlated with the induction of apoptosis by *Yersinia* (*5, 8, 9*).

The presence of YopJ-related proteins in other animal (AvrA of *Salmonella typhimurium*) and plant pathogens (AvrRxv of *Xanthamonas campestris* pv. *vesicatori*) as well as in a plant symbiont (Y4LO of *Rhizobium* NGR234) suggests that this family of proteins plays a fundamentally important role in bacterial-host cell interactions (*11, 12*). The amino acid sequence identity shared among YopJ, AvrA, AvrRxv, and Y4LO suggests that these effectors function through a common mechanism. However, a search for homologous proteins (by BLAST and other search programs) offers no insight into the function of this family of proteins.

To identify mammalian binding partners of YopJ, we used a yeast two-hybrid screen based on a LexA-YopJ fusion protein and a HeLa cDNA library (*13*). Positive clones were obtained, encoding fusion proteins of the Gal4 activation domain with MAPK kinases (MKK1, MKK2, and MKK4/SEK1) (Fig. 1A). These interactions were confirmed by cotransforming yeast cells with pLexAde-YopJ with purified plasmids, encoding fusions of the VP16 activation domain with full-length MKK1 or fusions of the Gal4 activation domain with MKK2 (Fig. 1A) (*14*). YopJ did not interact in the yeast two-hybrid system with MAPKs ERK, JNK, and p38 or with the MAPK kinase kinase (MAPKKK) BRaf, suggesting that the interaction of YopJ with the MKKs is specific (Fig. 1A) (*15*). To determine if YopJ could bind directly to MKKs in vitro, MKK1, MKK3, MKK4, and MKK5 were expressed as glutathione S-transferase (GST) fusion proteins in bacteria and tested for interaction with in vitro transcribed and translated ^{35}S-methionine–labeled YopJ. GST alone failed to bind YopJ, whereas all four GST-MKK fusion proteins bound labeled YopJ (Fig. 1B). Thus, YopJ was able to bind specifically to multiple members of the MKK family in vitro. To demonstrate that YopJ targets the MKKs in vivo, we coimmunoprecipitated YopJ with

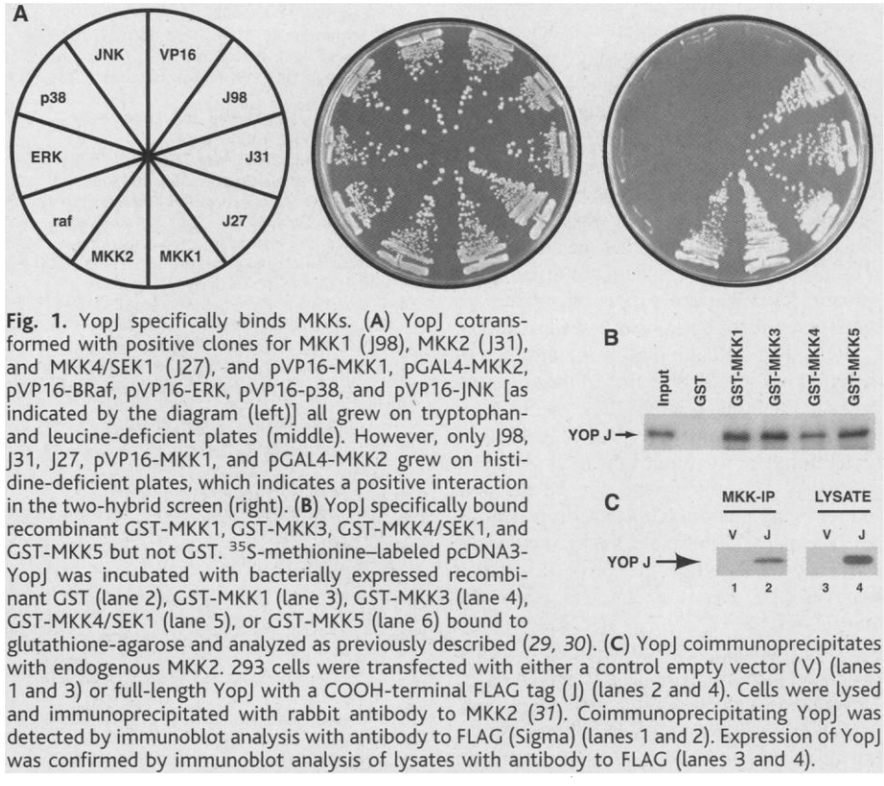

Fig. 1. YopJ specifically binds MKKs. (**A**) YopJ cotransformed with positive clones for MKK1 (J98), MKK2 (J31), and MKK4/SEK1 (J27), and pVP16-MKK1, pGAL4-MKK2, pVP16-BRaf, pVP16-ERK, pVP16-p38, and pVP16-JNK [as indicated by the diagram (left)] all grew on tryptophan- and leucine-deficient plates (middle). However, only J98, J31, J27, pVP16-MKK1, and pGAL4-MKK2 grew on histidine-deficient plates, which indicates a positive interaction in the two-hybrid screen (right). (**B**) YopJ specifically bound recombinant GST-MKK1, GST-MKK3, GST-MKK4/SEK1, and GST-MKK5 but not GST. ^{35}S-methionine–labeled pcDNA3-YopJ was incubated with bacterially expressed recombinant GST (lane 2), GST-MKK1 (lane 3), GST-MKK3 (lane 4), GST-MKK4/SEK1 (lane 5), or GST-MKK5 (lane 6) bound to glutathione-agarose and analyzed as previously described (*29, 30*). (**C**) YopJ coimmunoprecipitates with endogenous MKK2. 293 cells were transfected with either a control empty vector (V) (lanes 1 and 3) or full-length YopJ with a COOH-terminal FLAG tag (J) (lanes 2 and 4). Cells were lysed and immunoprecipitated with rabbit antibody to MKK2 (*31*). Coimmunoprecipitating YopJ was detected by immunoblot analysis with antibody to FLAG (Sigma) (lanes 1 and 2). Expression of YopJ was confirmed by immunoblot analysis of lysates with antibody to FLAG (lanes 3 and 4).

[1]Department of Biological Chemistry, University of Michigan, Ann Arbor, MI 48109–0606, USA. [2]Department of Molecular Genetics and Microbiology, [3]Center for Infectious Diseases, School of Medicine, State University of New York at Stony Brook, Stony Brook, NY 11794–5222, USA.

*Present address: Howard Hughes Medical Institute and Department of Immunology, University of Washington, Seattle, WA 98195, USA.

†Present address: Monsanto/Searle, 800 North Lindbergh Boulevard, St. Louis, MO 631667, USA.

‡To whom correspondence should be addressed. E-mail: jedixon@umich.edu

endogenous MKK2 from 293 cells (Fig. 1C).

To determine the biological consequences of YopJ binding to MKKs, we performed a series of biochemical experiments to assess the effect of YopJ on the MAPK pathway (Fig. 2). 293 cells were transfected with or without HA-ERK in the presence or absence of YopJ (*6*). Cells were stimulated with epidermal growth factor (EGF) and then assayed for ERK kinase activity by an immune complex assay in which myelin basic protein (MBP) was used as a substrate (*16*). EGF-treated cells transfected with HA-ERK displayed ERK activity; however, EGF-treated cells that were cotransfected with HA-ERK and YopJ displayed no ERK kinase activity (Fig. 2A). Therefore, YopJ blocked the MAPK pathway downstream of the EGF stimulus. Next, the effects of YopJ were assayed on ERK activity stimulated by activated Ras (HRasV12) (*16*). Cells transfected with HRasV12 displayed increase ERK activity, whereas cells transfected in the presence of YopJ displayed no ERK activity (Fig. 2B). A similar inhibitory effect of YopJ was observed when cells were transfected with activated Raf (v-Raf) (*16*), suggesting that YopJ was inhibiting the MAPK pathway downstream of the MAPKKK (that is, v-Raf) (Fig. 2C). In contrast, when cells were transfected with a constitutively active form of MKK1 (MKK1-ED) (*16*), robust ERK kinase activity was observed in either the presence or absence of YopJ (Fig. 2D). Therefore, YopJ was inhibiting the MAPK pathway downstream of EGF, Ras, and Raf and upstream of MKK1 (at the level of the MKK activation). These results demonstrate that the biological consequences of the in vitro and in vivo binding of MKKs to YopJ results in a specific block in the ability of Raf to stimulate MKK.

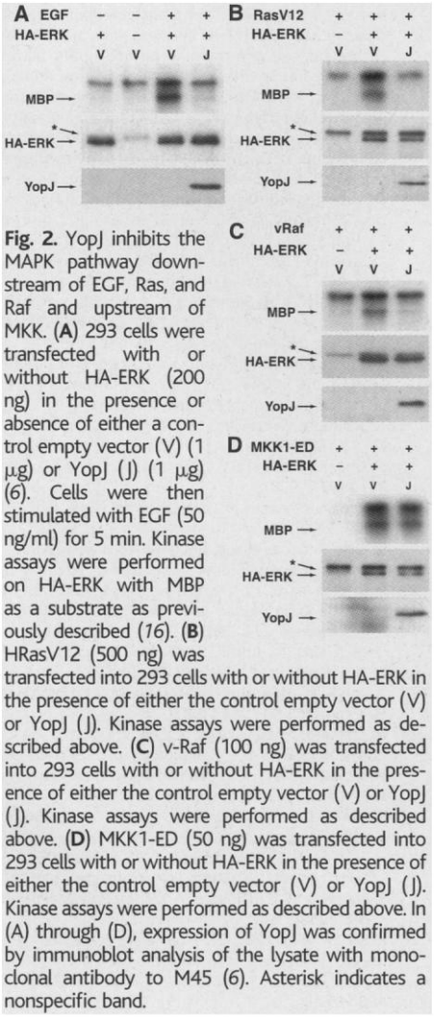

Fig. 2. YopJ inhibits the MAPK pathway downstream of EGF, Ras, and Raf and upstream of MKK. (**A**) 293 cells were transfected with or without HA-ERK (200 ng) in the presence or absence of either a control empty vector (V) (1 μg) or YopJ (J) (1 μg) (*6*). Cells were then stimulated with EGF (50 ng/ml) for 5 min. Kinase assays were performed on HA-ERK with MBP as a substrate as previously described (*16*). (**B**) HRasV12 (500 ng) was transfected into 293 cells with or without HA-ERK in the presence of either the control empty vector (V) or YopJ (J). Kinase assays were performed as described above. (**C**) v-Raf (100 ng) was transfected into 293 cells with or without HA-ERK in the presence of either the control empty vector (V) or YopJ (J). Kinase assays were performed as described above. (**D**) MKK1-ED (50 ng) was transfected into 293 cells with or without HA-ERK in the presence of either the control empty vector (V) or YopJ (J). Kinase assays were performed as described above. In (A) through (D), expression of YopJ was confirmed by immunoblot analysis of the lysate with monoclonal antibody to M45 (*6*). Asterisk indicates a nonspecific band.

Raf is known to function as a kinase that phosphorylates MKK1,2 on two serine residues, which results in MKK activation (*17, 18*). As expected, HA-MKK2 was phosphorylated when cells were stimulated with EGF, but no HA-MKK2 phosphorylation was observed in cells that were cotransfected with YopJ (Fig. 3A). As a result, YopJ prevented MKK2 from being activated by phosphorylation. Similarly, when MKK3 is activated by ultraviolet radiation, YopJ inhibits its phosporylation (*19*). The addition of YopJ to an in vitro kinase reaction with activated Raf and recombinant MKK1 did not result in a detectable inhibition of MKK phosphorylation, which suggests that an additional factor present in mammalian cells is required for inhibition of MKK phosphorylation (*19*). To determine if YopJ interfered with phosphorylation of MKKs in host cells infected with *Yersinia*, we infected murine macrophages with a wild-type or *yopJ*-mutant strain of *Y. pseudotuberculosis* and phosphorylation of MKK1,2 was assessed by immunoblotting. Both strains stimulated an initial robust, but transient, phosphorylation of MKK1,2 (Fig. 3B). At 45 min after infection [by which time YopJ had entered the cell (*20*)] the phosphorylation of MKK1,2 was significantly lower in cells infected with the wild-type strain than in those infected with the *yopJ*-mutant strain (Fig. 3B, lanes 3 and 5). Similar results were obtained when infected cells were analyzed for MKK4/SEK1 phosphorylation (*20*). These results demonstrate that YopJ inhibits MKK phosphorylation not only when YopJ is overexpressed in cells, but also when YopJ is delivered to the host cell through the type III secretion system.

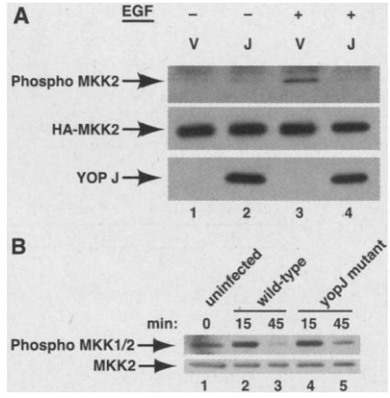

Fig. 3. YopJ inhibits phosphorylation of MKK2. (**A**) HA-MKK2 was transfected into 293 cells in the presence or absence of YopJ. Cells were then stimulated with EGF (50 ng/ml) for 5 min. Lysates were immunoprecipitated with antibody to HA, and phosphorylated MKK2 was detected by immunoblotting with antibody to phospho-specific MKK1/2 (New England Biolabs, Beverly, Massachusetts). Identical samples were immunoblotted with antibody to MKK2 to confirm equal expression (*31*). Immunoblotting with antibody to M45 confirmed expression of YopJ in lysates (*6*). (**B**) J774A.1 murine macrophage cells were left untreated or infected with wild-type or *yopJ*-mutant *Y. pseudotuberculosis* (*6*). At the indicated times, the macrophages were lysed in NP-40 buffer. Samples of the lysates adjusted to contain equivalent amounts of total protein were analyzed by immunoblotting (as described above) with antibody to phospho-specific MKK1/2 (top row) to detect phosphorylated MKK1/2 (P-MKK1/2) or antibody to MKK2 (bottom row) to confirm equal loading of MKK2. One experiment, representative of three, is shown.

Previous studies have demonstrated that macrophages infected by *Yersinia* are unable to elicit a proinflammatory response and subsequently die by apoptosis (*1*). The interaction of YopJ with MKK1, MKK3, MKK4, or MKK5 does not easily explain how this virulence factor could be affecting a proinflammatory or apoptotic response. Proinflammatory responses and the anti-apoptotic machinery are regulated by the NFκB pathway through the inhibitor of NF-κB (IκB) kinase complex, which in turn is regulated by upstream kinases (*21, 22*). The components of the IκB kinase complex that regulate the NFκB pathway include IKKα and IKKβ, which are activated by morphogenic signals and proinflammatory signals, respectively (*23*). In addition, recent studies have demonstrated that these kinases can be phosphorylated and activated by the MAPKKK, MEKK1 (*24, 25*). Figure 4D shows the parallel kinase cascades leading to MAPK and NFκB activation, where each step in the pathway contains a representative counterpart (that is, Raf and MEKK1, and MKK and IKKα or IKKβ). It was speculated that if YopJ recognized IKK as a MKK-like molecule and bound to it, the resulting interaction would result in inactivation of NFκB signaling. Therefore, we tested whether YopJ was able to inhibit the NFκB pathway downstream of MEKK1 by transfecting cells with an activated form of MEKK1 (ΔMEKK1) in the presence or absence of YopJ. Figure 4A shows that YopJ expression efficiently blocks the proinflammatory pathway downstream of MEKK1. It was next determined whether the IKKs, like the MKKs, could interact with YopJ. When labeled YopJ was incubated

with GST, GST-IKKα, GST-IKKβ, and GST-BRaf in vitro (*25, 26*), YopJ did not interact with GST, GST-IKKα, or GST-BRaf but did interact with GST-IKKβ (Fig. 4B). Proinflammatory signaling machinery targets activation of IKKβ but not IKKα (*23*), suggesting that the IKKβ contains distinct structural features that allow it to be recognized as a target by both the upstream proinflammatory signaling machinery (that is, MEKK1) and YopJ. Not only was an interaction observed with YopJ and IKKβ in vitro, but it was also found that YopJ was able to coprecipitate with IKKβ in vivo (Fig. 4C). These observations support the theory that YopJ is inhibiting both the NFκB pathway and the MAPK pathway downstream of MKKKs and upstream of MKKs through an interaction with the MKKs (Fig. 4D).

These results explain how a single bacterial protein, YopJ, prevents the activation of multiple downstream MKK controlled signaling pathways (Fig. 4). MKKs are a highly conserved family of proteins. As essential components of the MAPK signaling pathways, they are responsible for induction of cytokine production (*17, 27*). By targeting this conserved family of proteins, YopJ effectively shuts down the multiple kinase cascades that are required by the host cells to respond to a bacterial infection (*6, 7, 10*). As previously observed, addition of a dominant negative (inactive) form of IKKβ to mammalian cells results in inhibition of the NFκB pathway (*22*). Therefore, the finding that YopJ binds to IKKβ provides an explanation for the negative effect of YopJ on the proinflammatory pathway induced by NFκB, which uses a mechanism analogous to the one used in the MAPK pathways. In addition to its role as an activator of cytokine gene expression, NFκB regulates the synthesis of anti-apoptotic factors (*28*). Thus, by simultaneously blocking MAPK and NFκB signaling functions, YopJ blocks synthesis of cytokines as well as anti-apoptotic factors. In the absence of critical anti-apoptotic factors, apoptotic signals dominate, and programmed cell death ensues, unabated.

Together, these results have important implications for understanding the functions of the YopJ-related proteins found in bacteria that establish pathogenic or symbiotic relations with plants. In fact, the plant YopJ-related protein, AvrRxv, has been shown to induce an apoptotic-like program in plants, called the hypersensitive response (*11*). In conclusion, these results support the concept that YopJ is used by both plant and animal pathogens as well as by plant symbionts to modulate host signaling responses.

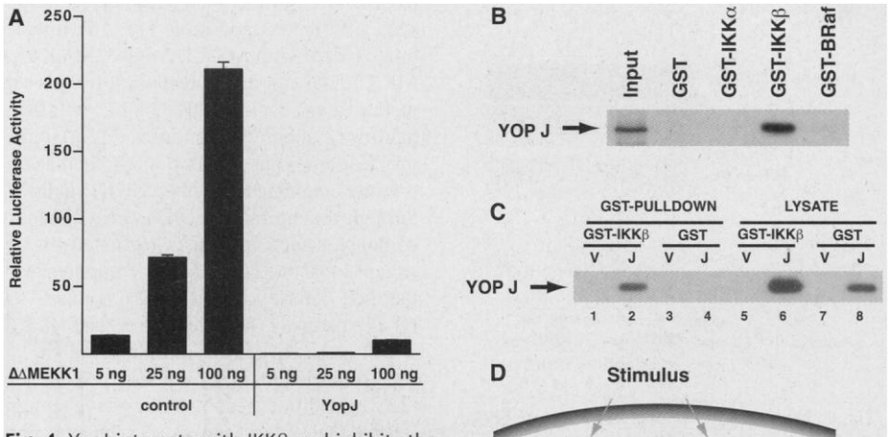

Fig. 4. YopJ interacts with IKKβ and inhibits the NFκB pathway downstream of MEKK1. (**A**) YopJ inhibits the NFκB pathway downstream of MEKK1. Cells were transfected with increasing concentrations of MEKK1 (as indicated) with a pCMV-lacZ (0.5 μg) plasmid and pNFκB-Luc reporter plasmid (0.1 μg) (Stratagene, La Jolla, California) in the presence or absence of YopJ (1 μg). (**B**) YopJ specifically binds GST-IKKβ but not GST-IKKα, GST-BRaf, or GST. pEBG-3X (lane 2), pEBG-3X-IKKα (lane 3), pEBG-3X-IKKβ (lane 4), and pEBG-3X-BRaf (lane 5) were expressed in 293 cells. Cells were lysed, and GST fusion proteins were isolated with glutathione-agarose. ^{35}S-methionine–labeled YopJ was incubated with the equivalent amounts of GST fusion proteins and analyzed as previously described (*25, 29*). (**C**) YopJ coimmunoprecipitates with transiently expressed GST-IKKβ. pEBG-3X-IKKβ (lanes 1, 2, 5, and 6) or pEBG-3X (lanes 3, 4, 7, and 8) (*25*) were transfected into 293 cells in the presence of either a control empty vector or a FLAG-tagged YopJ. GST fusion proteins were isolated, and bound YopJ was detected by immunoblot analysis. Expression of YopJ was confirmed by immunoblot analysis of lysates with antibody to FLAG (lanes 5, 6, 7, and 8). (**D**) YopJ inhibits all pathways that utilize MKKs for signaling, including ERK, p38, and JNK pathways, and YopJ also inhibits the NFκB pathway. The inhibition results in a block of a proinflammatory response and of anti-apoptotic factor expression, thereby promoting programmed cell death.

References and Notes

1. R. R. Brubaker, *Curr. Top. Microbiol. Immunol.* **57**, 111 (1972); G. R. Cornelis *et al.*, *Microbiol. Mol. Biol. Rev.* **62**, 1315 (1998).
2. L. E. Palmer, S. Hobbie, J. E. Galan, J. B. Bliska, *Mol. Microbiol.* **27**, 953 (1998).
3. S. C. Straley, E. Skrzypek, G. V. Plano, J. B. Bliska, *Infect. Immun.* **61**, 3105 (1993).
4. D. M. Monack, J. Mecsas, D. Bouley, S. Falkow, *J. Exp. Med.* **188**, 2127 (1998).
5. S. D. Mills *et al.*, *Proc. Natl. Acad. Sci. U.S.A.* **94**, 12638 (1997).
6. L. E. Palmer, A. R. Pancetti, S. Greenberg, J. B. Bliska, *Infect. Immun.* **67**, 708 (1999).
7. A. Boland and G. R. Cornelis, *ibid.* **66**, 1878 (1998).
8. K. Schesser *et al.*, *Mol. Microbiol.* **28**, 1067 (1998).
9. D. M. Monack, J. Mecsas, N. Ghori, S. Falkow, *Proc. Natl. Acad. Sci. U.S.A.* **94**, 10385 (1997).
10. K. Ruckdeschel *et al.*, *J. Exp. Med.* **187**, 1069 (1998).
11. M. C. Whalen *et al.*, *Mol. Plant-Microbe Interact.* **6**, 616 (1993).
12. L. D. Ciesiolka *et al.*, *ibid.* **12**, 35 (1999); C. Freiberg *et al.*, *Nature* **387**, 394 (1997); W. D. Hardt and J. E. Galan, *Proc. Natl. Acad. Sci. U.S.A.* **94**, 9887 (1997); M. C. Whalen, R. E. Stall, B. J. Staskawicz, *ibid.* **85**, 6743 (1988).
13. A. B. Vojtek and S. M. Hollenberg, *Methods Enzymol.* **255**, 331 (1995). Full-length YopJ was fused in-frame into pLexAde and transfected into the L40 reporter stain. This cell line was then transfected with HeLa cell polythymine-primed cDNA library cloned in-frame with the GAL4 activation domain (Clontech, Palo Alto, CA), and 3 million transformants (about three times the library complexity) were assayed for a positive two-hybrid interaction on histidine-deficient plates, followed by confirmation with a β-galactosidase filter assay. Positive clones encoded fusion proteins of the Gal4 activation domain with MKK1 (J98, initiating at glycine 61), MKK2 (J31, J62, and J22, initiating at glycine 29, glycine 29, and glutamine 32, respectively), and MKK4 (J27, initiating at glutamine 38).
14. P. M. Holland, M. Suzanne, J. S. Campbell, S. Noselli, J. A. Cooper, *J. Biol. Chem.* **272**, 24994 (1997); S. Stewart *et al.*, *Mol. Cell. Biol.* **19**, 5523 (1999).
15. A. J. Waskiewicz, A. Flynn, C. G. Proud, J. A. Cooper, *EMBO J.* **16**, 1909 (1997); pVP16-BRaf was a generous gift from C. Figueroa and A. Vojtek.
16. T. Sugimoto, S. Stewart, M. Han, K. L. Guan, *EMBO J.* **17**, 1717 (1998).
17. N. Dhanasekaran and E. Premkumar Reddy, *Oncogene* **17**, 1447 (1998).
18. H. J. Schaeffer and M. J. Weber, *Mol. Cell. Biol.* **19**, 2435 (1999).
19. K. Orth and J. E. Dixon, unpublished observation.
20. L. E. Palmer and J. B. Bliska, unpublished observation.
21. J. A. DiDonato, M. Hayakawa, D. M. Rothwarf, E. Zandi, M. Karin, *Nature* **388**, 548 (1997); F. Mercurio *et al.*, *Science* **278**, 860 (1997); J. D. Woronicz, X. Gao, Z. Cao, M. Rothe, D. V. Goeddel, *ibid.*, p. 866; C. H. Regnier *et al.*, *Cell* **90**, 373 (1997).
22. E. Zandi, D. M. Rothwarf, M. Delhase, M. Hayakawa, M. Karin, *Cell* **91**, 243 (1997).
23. M. Delhase, M. Hayakawa, Y. Chen, M. Karin, *Science* **284**, 309 (1999); Y. Hu *et al.*, *ibid.*, p. 316; K. Takeda *et al.*, *ibid.*, p. 313; Q. Li, D. Van Antwerp, F. Mercurio, K.-F. Lee, I. M. Verma, *ibid.*, p. 321.
24. M. J. Yin, Y. Yamamoto, R. B. Gaynor, *Nature* **396**, 77 (1998); M. J. Yin *et al.*, *Cell* **93**, 875 (1998); H. Nakano *et al.*, *Proc. Natl. Acad. Sci. U.S.A.* **95**, 3537 (1998); F. S. Lee, R. T. Peters, L. C. Dang, T. Maniatis, *ibid.*, p. 9319.
25. S. Nemoto, J. A. DiDonato, A. Lin, *Mol. Cell. Biol.* **18**, 7336 (1998).
26. pEBG-3X and pEBG-3X-BRaf were generous gifts from C. Figueroa and A. Vojtek.
27. B. Li, C. Tournier, R. J. Davis, R. A. Flavell, *EMBO J.* **18**, 420 (1999).

28. C.-Y. Wang, M. W. Mayo, R. G. Korneluk, D. V. Goeddel, A. S. Baldwin Jr., *Science* **281**, 1680 (1998).
29. G. Zhou, Z. Q. Bao, J. E. Dixon, *J. Biol. Chem.* **270**, 12665 (1995).
30. pGEX-2T-MKK4/SEK1 was a generous gift from J. Woodgett; pGEX2T-MKK3 was a generous gift from T. Sugimoto and K.-L. Guan.
31. C. F. Zheng and K. L. Guan, *J. Biol. Chem.* **269**, 19947 (1994).
32. We thank C. Worby, J. Clemens, T. Maehama, M. Muda, S. Juris, I. Jones, C. Figueroa, and other members of the Dixon lab for stimulating discussions and technical support. We are very grateful to A. Vojtek, K.-L. Guan, Z. Xu, and members of their lab for their generous support and assistance. In addition, we are grateful to A. Lin, J. Woodgett, and M. Cobb for their generous supply of reagents. This work was funded by NIH grants 18024 (J.E.D.) and AI35175 (J.B.B.) and the Walther Cancer Institute (J.E.D. and K.O.).

13 May 1999; accepted 19 August 1999

Synergy Between Tumor Suppressor *APC* and the β-Catenin–Tcf4 Target *Tcf1*

Jeroen Roose,[1]* Gerwin Huls,[1]* Moniek van Beest,[1]* Petra Moerer,[1] Karin van der Horn,[1] Roel Goldschmeding,[3] Ton Logtenberg,[1] Hans Clevers[1,2]†

Mutations in APC or β-catenin inappropriately activate the transcription factor Tcf4, thereby transforming intestinal epithelial cells. Here it is shown that one of the target genes of Tcf4 in epithelial cells is *Tcf1*. The most abundant Tcf1 isoforms lack a β-catenin interaction domain. *Tcf1*$^{-/-}$ mice develop adenomas in the gut and mammary glands. Introduction of a mutant APC allele into these mice substantially increases the number of these adenomas. Tcf1 may act as a feedback repressor of β-catenin–Tcf4 target genes and thus may cooperate with APC to suppress malignant transformation of epithelial cells.

The tumor suppressor gene *APC*, first identified in a dominantly inherited disorder termed familial adenomatous polyposis, is mutated in the vast majority of colorectal cancers (*1*). APC's principal role is that of a negative regulator of the Wnt signal transduction cascade (*2*). APC resides in a large complex with axin, GSK3, and the Wnt effector β-catenin (*3*). In this complex, the serine kinase GSK-3β constitutively phosphorylates β-catenin at a set of regulatory NH_2-terminal Ser/Thr residues, thereby targeting β-catenin for ubiquitination by β-TrCP and for subsequent proteasomal degradation (*4*). Wnt signaling stabilizes β-catenin. In the nucleus, β-catenin binds to Tcf/Lef transcription factors. The bipartite complex then activates transcription of Tcf target genes (*5*). In the absence of signaling, Tcf factors repress transcription by interaction with Groucho transcriptional repressors or with CBP (*6*).

Loss of *APC* leads to the nuclear accumulation of β-catenin, which constitutively binds to Tcf4 (*7*), a Tcf family member specifically expressed in epithelia of the intestine and mammary gland (*8*). In some colorectal cancers that carry wild-type *APC* as well as in several other types of cancer, dominant mutations alter one of the four regulatory NH_2-terminal Ser/Thr residues of β-catenin. This also leads to the inappropriate formation of β-catenin–Tcf complexes in the nucleus (*9*).

Expression of *Tcf1*, a gene encoding another Tcf family member, is largely restricted to T lineage lymphocytes in adult tissues and cell lines (*10*). However, colorectal cell lines have also been reported to express appreciable amounts of *Tcf1* (*11*). Confirming the latter observation, we detected *Tcf1* mRNA by Northern (RNA) blot analysis in five of six colorectal cell lines (*12*). Three of these are *APC* mutants (SW480, HT-29, and DLD1), and two others (LS174T and HCT116), carry oncogenic mutations in β-catenin. The cell line that did not express *Tcf1* (RKO) is wild-type for both *APC* and β-catenin, suggesting that *Tcf1* expression might normally be regulated by these genes. We also detected nuclear Tcf1 protein in normal human tissues: in proliferating intestinal epithelial cells and in the basal epithelial cells of mammary gland epithelium (*13*) (Fig. 1). The most abundant Tcf1 isoforms lack a β-catenin interaction domain (*10*). Because they retain their Groucho interaction domain, they are likely to act as negative regulators of Wnt signaling.

To test whether *Tcf1* is a target of Tcf4, we used a transfectant derived from the APC$^{-/-}$ HT29 cell line, which inducibly expresses wild-type APC (*14*). This transfectant previously allowed the identification of another Tcf4 target, c-*Myc* (*15*). APC expression was induced in HT29-APC cells for 20 hours. The cells remained attached and were >95% viable. Northern (RNA) blot analysis revealed a consistent four- to fivefold decrease in steady-state mRNA levels for *Tcf1* and c-*Myc* (Fig. 2A), but no changes in the levels of *Ep-Cam* and γ-*actin* mRNAs. This experiment indicated that *Tcf1* is regulated by APC, and therefore by β-catenin–Tcf4.

The human *Tcf1* gene is transcribed from two closely spaced promoters (*10*). We sequenced 1.2 kb directly upstream of promoter I and found the region to be a CpG island containing two potential Tcf-binding motifs (Fig. 2B). The region acted as an enhancer, both in the context of promoter I and of a heterologous promoter (*12*). We tested the inducibility of the putative enhancer fragment by β-catenin and Tcf expression constructs in our "model" B cell line IIA1.6, which lacks endogenous Tcf/Lef factors (*7*, *16*). The combination of β-catenin and Tcf4 transactivated the enhancer three- to fourfold in a transient reporter assay (Fig. 2C). Furthermore, expression of a dominant-negative Tcf4 (ΔNTcf4, which lacks the β-catenin interaction domain) inhibited enhancer activity in LS174T colorectal cancer cells (Fig. 2D).

Tcf1-deficient mice develop a progressive block in early thymocyte development (*17*). Nevertheless, *Tcf1*$^{-/-}$ mice have functional peripheral T cells, are fully immunocompetent, and live for over a year (*18*). Prompted by a possible link between Tcf4 activity and *Tcf1* expression in the intestine, we performed autopsies on *Tcf1*$^{-/-}$ mice of various ages. Unexpectedly, we observed mammary gland adenomas and polyplike intestinal neoplasms in these mice (Fig. 3A). These lesions

Table 1. *Min/+Tcf1*$^{-/-}$ mice demonstrated a 10-fold increase in the formation of intestinal neoplasms compared with *Min/+* mice. ND, not done (mice were killed at 4 months).

Genotype	Age (months)	No. of neoplasms in small intestine (mean ± 1 SD)	No. of neoplasms in colon (mean ± 1 SD)
Min/+Tcf1$^{+/+}$	3	9 ± 3 (n = 9)	0.5 ± 1 (n = 9)
Min/+Tcf1$^{-/-}$	3	102 ± 10 (n = 9)	11.0 ± 3 (n = 9)
Min/+Tcf1$^{+/+}$	5–6	35 ± 13 (n = 7)	1.1 ± 1.1 (n = 7)
Min/+Tcf1$^{+/-}$	5–6	48 ± 15 (n = 7)	3.2 ± 2.2 (n = 7)
Min/+Tcf1$^{-/-}$	5–6	ND	ND

[1]Department of Immunology and [2]Center for Biomedical Genetics, [3]Department of Pathology, University Medical Center Utrecht, Post Office Box 85500, 3508 GA Utrecht, Netherlands.

*These authors contributed equally to this work.
†To whom correspondence should be addressed. E-mail: h.clevers@lab.azu.nl